

Enhanced sensitivity of Z-scan technique by use of flat-topped beam

J. Wang · B. Gu · Y.M. Xu · H.T. Wang

Received: 23 October 2008 / Revised version: 2 April 2009 / Published online: 2 May 2009
© Springer-Verlag 2009

Abstract Based on the Huygens–Fresnel diffraction integral method, we report a theoretical investigation on the closed-aperture Z-scan technique by using the flat-topped beam. The sensitivity of the flat-topped beam Z-scan technique, which can be enhanced with the increase of the flatness order N for the flat-topped beam, is greatly higher than of the Gaussian beam. Some salient characteristics of the flat-topped beam Z-scan traces are addressed. The flat-topped beam Z-scan technique for characterizing the instantaneous nonlinearity is also presented.

PACS 42.65.An · 42.25.Bs · 42.70.Jk

1 Introduction

Since the Z-scan technique by the use of the Gaussian beam was firstly pioneered [1], the Z-scan technique has been extensively used as an important tool to explore the optical nonlinearities of materials. Subsequently, several modified Z-scan techniques by the use of various non-Gaussian beams have been presented, such as by using the Gaussian–Bessel beam [2], the top-hat beam [3], the quasi-one-dimensional slit beam [4], the Laguerre–Gaussian beam [5], and the flat-topped beam [6].

Besides the Z-scan measurement, the flat-topped beam has also many potential applications including optical processing, inertial confinement fusion, sorting and imaging, tracking, and long-distance optical communication [7]. A number of devices could be used to produce the flat-topped beam from a Gaussian beam, such as filters and diffractive elements. Xie et al. presented a Fabry–Perot etalon with angular dependence of the transmission characteristic to produce a flatten beam [8]. Veldkamp showed a technique to obtain a flat-topped distribution beam by modulating only the phase of the laser beam between two binary values [9]. Hoffnagle et al. designed a refractive optical system to convert a Gaussian beam to a flat-topped beam [10]. Furthermore, some models for describing the flat-topped beam have been proposed, for example, the super-Gaussian beam model [11], the flattened Gaussian beam model [12], the multi-Gaussian beam model [13], and the model composed of lower-order Gaussian modes [14, 15]. In [6], the nonlinear absorption of materials was investigated by the use of the open-aperture flat-topped Z scan.

In the present article, we explore the sensitivity enhancement of the closed-aperture Z-scan technique by using the flat-topped beam for characterizing the nonlinear refraction of the optically thin sample. Based on the Huygens–Fresnel integral method, we give the numerical simulations of the Z-scan traces. We verify that the sensitivity of the flat-topped beam Z scan is dramatically improved with respect to the Gaussian beam Z scan as the flatness order N increases. Some salient features of the flat-topped beam Z scan are discussed in detail. We also extend this Z-scan scheme for characterizing the optical nonlinearity from the steady state to instantaneous case.

J. Wang · Y.M. Xu · H.T. Wang (✉)
Nanjing National Laboratory of Microstructures and Department
of Physics, Nanjing University, Nanjing 210093, China
e-mail: htwang@nju.edu.cn

B. Gu
Jiangsu Key Laboratory on Opto-Electronic Technology and
Department of Physics, Nanjing Normal University,
Nanjing 210097, China

2 Theoretical foundation

There are many models for describing the flat-topped beam, such as the super-Gaussian beam model, the flattened Gaussian beam model, and the model composed of lower-order Gaussian modes [11–15]. On the basis of the model developed in [14, 15], the flat-topped beam can be written as

$$F(r) = \sum_{n=1}^N \frac{(-1)^{n-1}}{N} \binom{N}{n} \exp(-nr^2), \quad (1)$$

where r is the radial coordinate and N is referred as the flatness order for the flat-topped beam. Assuming a flat-topped beam propagating along the $+z$ direction, which is composed of finite number of the fundamental Gaussian modes with different beam waists, the electric field can be expressed as follows [14]

$$E(z, r) = \frac{\left[\sum_{n=1}^N \frac{(-1)^{n-1}}{N} \binom{N}{n} \frac{\omega_{n0}}{\omega_{nz}} \exp\left(-\frac{r^2}{\omega_{nz}^2} - \frac{ikr^2}{2R_{nz}}\right) \right]}{\sum_{n=1}^N \frac{(-1)^{n-1}}{N} \binom{N}{n}}, \quad (2)$$

where

$$\omega_{n0} = \omega_0 n^{-1/2}, \quad (3)$$

$$z_{n0} = k\omega_{n0}^2/2, \quad (4)$$

$$\omega_{nz} = \omega_{n0} [1 + (z/z_{n0})^2]^{1/2}, \quad (5)$$

$$R_{nz} = z [1 + (z_{n0}/z)^2]. \quad (6)$$

Here λ and $k = 2\pi/\lambda$ are the wavelength and the wavenumber of the used laser in free space, respectively; ω_{n0} , z_{n0} , ω_{nz} , and R_{nz} are the beam waist, the Rayleigh length, the beam radius at the z plane, and the radius of curvature of the wavefront at the z plane for the n th order component of the flat-topped beam, respectively. It should be noted that (1) degenerates into a TEM₀₀ Gaussian beam when taking $N = 1$.

The scheme of the flat-topped beam Z scan is shown by the inset of Fig. 1. A flat-topped beam propagates along the $+z$ axis within an optically thin medium with linear absorption coefficient α and third-order nonlinear refraction coefficient γ . When the sample is located at a position z , the complex optical field $E(r, z; t)$ at the input plane of the sample should be rewritten as, in the general case

$$E(r, z; t) = E(r, z) \sqrt{\rho(t)}, \quad (7)$$

where $\rho(t)$ describes the temporal profile of the laser pulses used in the Z-scan measurement. Two widely used pulse profiles are $\rho(t) = \exp(-t^2/\tau^2)$ for Gaussian and $\rho(t) = \text{sech}^2(t/\tau)$ for hyperbolic secant profiles, where τ is the e^{-1} pulse half width for both types of pulses. Under the excitation of the continuous wave (CW) laser or the steady-state

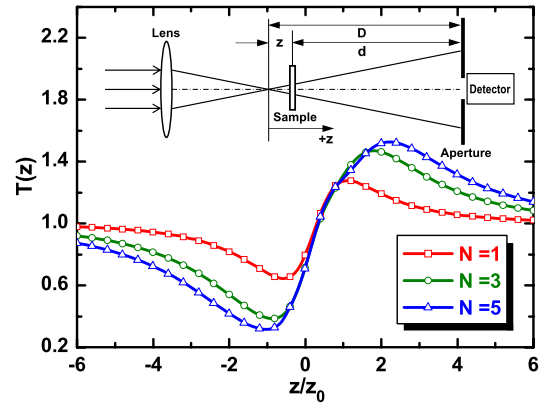


Fig. 1 Dependences of the flat-topped beam Z-scan traces on the flatness order N for $S = 0.05$ and $\Phi_0 = 0.5\pi$. The inset is the schematic diagram of the Z-scan technique

condition, $\rho(t)$ is always unity. The complex electric field $E_e(r, z; t)$ at the exit plane of the sample can be given, in terms of the field $E(r, z; t)$ at the incident plane of the sample

$$E_e(r, z; t) = E(r, z; t) \exp(-\alpha L/2) \times \exp[ikL_{\text{eff}}\gamma |E(r, z; t)|^2], \quad (8)$$

where $L_{\text{eff}} = [1 - \exp(-\alpha L)]/\alpha$ and L are the effective and the physical thickness of the sample, respectively. When the sample is located at the focal plane $z = 0$, the nonlinear phase shift caused by nonlinear refraction effect at $r = 0$ is $\Phi_0 = k\gamma I_0 L_{\text{eff}}$, where I_0 is the on-axis peak intensity at the focal plane.

We now consider the propagation of the optical field $E_e(r, z; t)$ from the exit plane of the sample to the plane of the far-field aperture. The far-field aperture has a distance of d with respect to the focal plane, the sample and the far-field aperture has a distance of D ($D = d - z$), where z denotes the sample position with respect to the focal plane ($z = 0$) and is positive when the sample is located at the right side of the focal plane. We assume the Fresnel approximations to be valid (under the far-field condition, in general, $d \geq 20z_0$), and $E_a(r_a, z; t)$ or $E_a(x_a, y_a, z; t)$ can be express in terms of $E_e(r, z; t)$ or $E_e(x, y, z; t)$, as follows [16]

$$E_a(x_a, y_a, z; t) = \frac{\exp(ikD)}{i\lambda(d-z)} \times \int_{-\infty}^{\infty} \int_{-\infty}^{\infty} E_e(x, y, z; t) \times \exp \frac{i\pi[(x_a - x)^2 + (y_a - y)^2]}{\lambda D} dx dy, \quad (9)$$

where (x, y) and (x_a, y_a) are the Cartesian coordinates attached to the sample plane and the far-field aperture plane,

and r and r_a are the radial coordinate in the corresponding planes, respectively, with $r^2 = x^2 + y^2$ and $r_a^2 = x_a^2 + y_a^2$. By the use of the Hankel transfer [16–18], the field distribution at the plane of the far-field aperture, $E_a(r_a, z; t)$, can be expressed in terms of $E_e(r, z; t)$, as follows [16]

$$\begin{aligned} E_a(r_a, z; t) &= \frac{2\pi \exp[i\pi r_a^2/\lambda(d-z)]}{i\lambda(d-z)} \\ &\times \int_0^\infty r E_e(r, z; t) \exp\left[\frac{i\pi r^2}{\lambda(d-z)}\right] \\ &\times J_0\left[\frac{2\pi rr_a}{\lambda(d-z)}\right] dr, \end{aligned} \quad (10)$$

where $J_0(\cdot)$ is the Bessel function of zero order. Thus the normalized Z-scan transmittance $T(z)$ can be easily rewritten as

$$T(z) = \frac{\int_{-\infty}^\infty dt \int_0^{R_a} r_a dr_a |E_a(r_a, z; t)|^2}{\int_{-\infty}^\infty dt \int_0^{R_a} r_a dr_a |E_a(r_a, z; t)|^2|_{\Phi_0=0}}, \quad (11)$$

where R_a is the radius of the far-field aperture. For the CW laser and steady-state case, i.e., $\rho(t) = 1$, (9) and (10) degenerate into, respectively

$$\begin{aligned} E_e(r, z) &= E(r, z) \exp(-\alpha L/2) \\ &\times \exp[ikL_{\text{eff}}\gamma |E(r, z)|^2], \end{aligned} \quad (12)$$

$$\begin{aligned} E_a(r_a, z) &= \frac{2\pi \exp[i\pi r_a^2/\lambda(d-z)]}{i\lambda(d-z)} \\ &\times \int_0^\infty r E_e(r, z) \exp\left[\frac{i\pi r^2}{\lambda(d-z)}\right] \\ &\times J_0\left[\frac{2\pi rr_a}{\lambda(d-z)}\right] dr. \end{aligned} \quad (13)$$

Correspondingly, (11) is simplified as

$$T(z) = \frac{\int_0^{R_a} r_a dr_a |E_a(r_a, z)|^2}{\int_0^{R_a} r_a dr_a |E_a(r_a, z)|^2|_{\Phi_0=0}}. \quad (14)$$

Thus we use (12)–(14) to perform the numerical simulations of the CW or steady-state case.

3 Analysis and discussion

We now numerically investigate the characteristics of the Z-scan traces under the steady-state condition. As an example, Fig. 1 shows the flat-topped beam Z-scan traces for different flatness order N with $S = 0.05$ and $\Phi_0 = 0.5\pi$. The parameter S is the linear transmittance of the far-field aperture in the Z-scan scheme. For the sake of comparison, we also plot the conventional Gaussian beam Z-scan trace (i.e.,

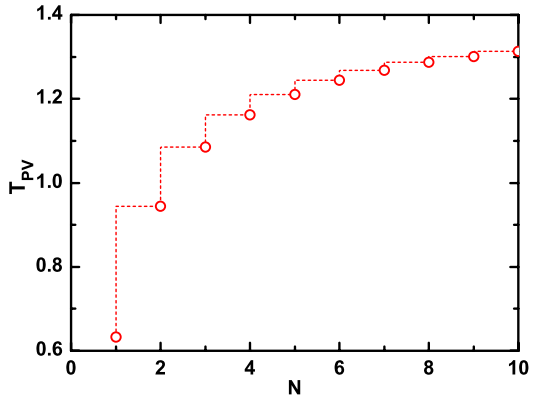


Fig. 2 The sensitivity of the flat-topped beam Z scan, T_{PV} , as a function of the flatness order N for $S = 0.05$ and $\Phi = 0.5\pi$

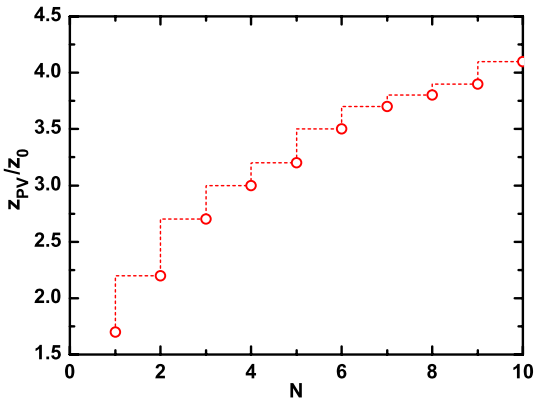


Fig. 3 The separation between the peak and the valley, Z_{PV}/Z_0 , as a function of the flatness order N for $S = 0.05$ and $\Phi = 0.5\pi$

the case of $N = 1$). One can see that the peak height ($T_P - 1$) and the valley depth ($1 - T_V$) synchronously enhance as the flatness order N increases, where T_P and T_V are the normalized peak and valley transmittances in the flat-topped Z-scan trace, respectively. Therefore, the normalized peak–valley transmittance difference $T_{PV} = T_P - T_V$ depends strongly on N . Here we define the separation between the peak and the valley to be Z_{PV} . Figures 2 and 3 plot T_{PV} and Z_{PV} as functions of N for $S = 0.05$ and $\Phi_0 = 0.5\pi$, respectively. It can be seen that when the flat-topped beam degenerates into a TEM₀₀ Gaussian beam ($N = 1$), we find $T_{PV} = 0.406\Phi_0$ and $Z_{PV} \sim 1.7z_0$, which are in good agreement with the results reported previously [19]. As N increases, the sensitivity of the flat-topped beam Z scan increases dramatically in the case of smaller N while increases slowly in the case of larger N , as shown in Fig. 2. One can also see that Z_{PV} enlarges as N increases, for instance, $Z_{PV} \sim 4.2z_0$ when $N = 10$, as shown in Fig. 3.

As examples, the flat-topped Z-scan traces for different values of Φ_0 when $N = 5$ and $S = 0.05$ are investigated and shown in Fig. 4. The peak and valley in the Z-scan traces are enhanced synchronously as Φ_0 increases. Furthermore,

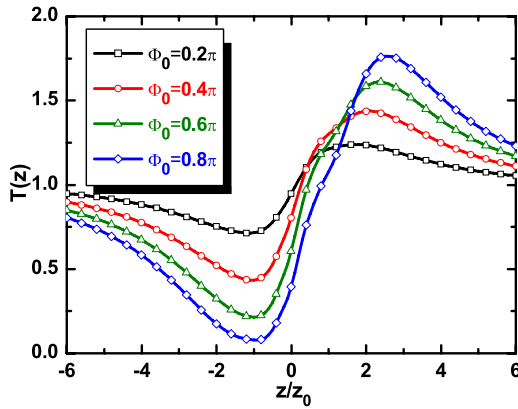


Fig. 4 The flat-topped beam Z-scan traces for $N = 5$ and $S = 0.05$ at different values of Φ_0

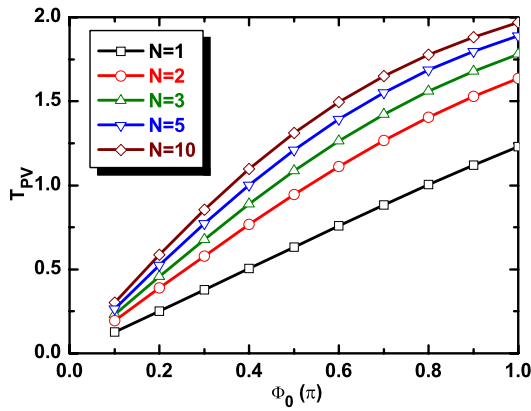


Fig. 5 The sensitivity of the flat-topped beam Z-scan, T_{PV} , as a function of Φ_0 for $S = 0.05$ and for different N

the peak position is almost independent of Φ_0 while the valley is away from the focal plane as Φ_0 increases. Figure 5 plots T_{PV} as a function of Φ_0 for different values of N when $S = 0.05$. We find that T_{PV} of the Gaussian beam Z-scan ($N = 1$) exhibits the near-linear growth as Φ_0 increases, which is consistent with the result reported previously. However, T_{PV} of the flat-topped beam Z scan ($N > 1$) becomes the nonlinear growth as Φ_0 increases.

Figure 6 shows the dependence of the flat-topped Z-scan traces on the linear transmittance S of the far-field aperture when $N = 2$ and $\Phi_0 = 0.5\pi$. Numerical simulation results reveal: (1) the magnitudes of the peak and the valley in the flat-topped beam Z-scan trace decrease as S increases; (2) the magnitude reduction of the peak is more rapid than that of the valley as S increases. Figure 7 plots T_{PV} versus S , when $N = 2$ and $\Phi_0 = 0.5\pi$. It can be seen that T_{PV} nonlinearily decreases as S increases. Therefore, to enhance the sensitivity of the flat-topped beam Z-scan measurement, the value of S should be as small as possible. However, it should be noted that the too small S will give rise to the large perturbation. Therefore, in the practical measurements,

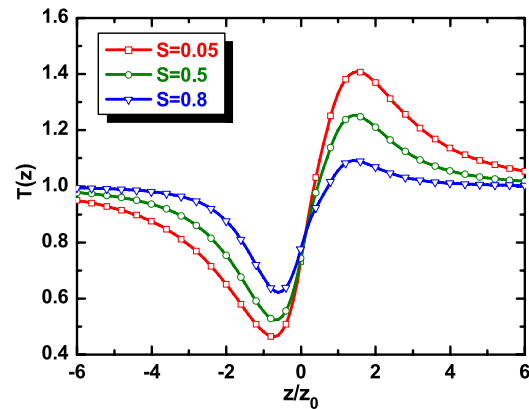


Fig. 6 Influence of the linear transmittance S of the far-field aperture on the flat-topped beam Z-scan traces with $N = 2$ and $\Phi_0 = 0.5\pi$

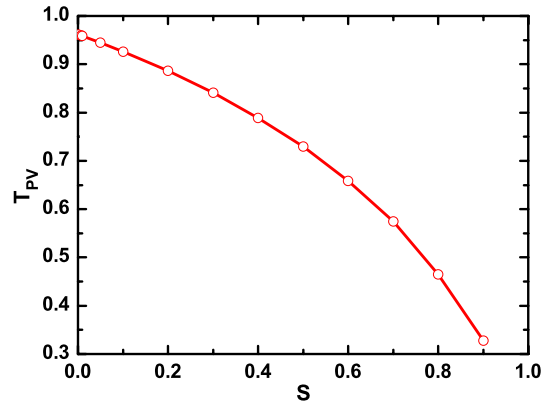


Fig. 7 Dependence of the sensitivity of the flat-topped beam Z-scan, T_{PV} , on the linear transmittance S for $N = 2$ and $\Phi_0 = 0.5\pi$

S should be chosen to be a suitable or eclectic value, such as $S = 0.1$.

We only consider the steady state case (the input laser pulse width is much larger than the response time of nonlinear materials) or the CW excitation case so far, in which $\rho(t)$ is always unity. However, there exists often the situation that the pulse duration of the laser pulses is close to or smaller than the response time of nonlinear materials. So, it is necessary to consider the influence of the temporal profile of the laser pulses on the Z-scan curves under the excitation of ultrafast-pulsed lasers. To explore the ultrafast physical property and to determine the intrinsic optical nonlinearity of a material, the Z-scan measurement is usually performed with the ultrafast laser pulses with low repetition rate. Here we deal with a situation that the pulse duration of the laser used is much shorter than the characteristic response time of the nonlinear sample. In this transient situation, the nonlinear response of the sample depends on the transient intensity of the laser pulses. Consequently, the temporal profile of the laser pulses used in the Z-scan measurement should be considered. As an exam-

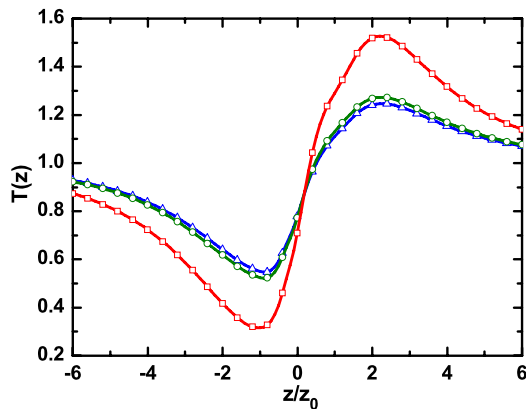


Fig. 8 The flat-topped beam Z-scan traces for a CW laser (squares), a Gaussian-shape pulsed laser (circles), and a hyperbolic-secant-squared pulsed laser (triangles) when $N = 5$, $\Phi_0 = 0.5\pi$, and $S = 0.05$

ple, we numerically simulate the flat-topped beam Z-scan traces with $N = 5$, $\Phi_0 = 0.5\pi$, and $S = 0.05$. For the laser pulses with the Gaussian- and hyperbolic-secant temporal profiles, the simulated results are plotted by the circles and triangles, respectively, as shown in Fig. 8. For comparison, the Z-scan trace for the CW laser is also presented in Fig. 8 by the squares. It can be found that the Z-scan traces under the excitation of the Gaussian- and hyperbolic-secant temporal pulses have the negligible difference but exhibit the great difference from that in the excitation of the CW laser. Therefore, carrying out the flat-topped beam Z-scan measurements under the excitation of ultrafast-pulsed lasers, one also should take into account the temporal profile of the laser pulses. It is of great interest why the CW and pulse lasers have significant difference in the Z-scan trace. For the CW excitation, the lens-like induced by the CW laser inside the sample is time-independent or invariable. In contrast, for the pulse excitation, the lens-like induced by the pulse laser is time-dependent or instantaneous, that is to say, the lens-like experiences a process from creating to demolishing (the behavior of the time evolution exhibits the same temporal profile as the laser pulses). It is easily understood that the CW laser Z scan is higher in sensitivity than the pulse laser, as shown in Fig. 7. So, it is necessary to consider the influence of the temporal behavior of the laser pulses on the Z-scan curves under the excitation of pulse lasers.

In addition, two problems should be of importance and of interest. First one is how to determine the value of N for the flat-topped beam used in the practical experiments. In fact, the value of N should be precisely identified before applying the presented Z-scan theory. If the flat-topped beam is to be generated like in [8–10], of course, the value of N becomes to be known. Even though the value of N for the flat-topped beam is unknown, N can be still determined through the agency of the knife edge or other methods and the best fitting between the flat-topped beam and the measured spatial

intensity profile. Second one is how to estimate the nonlinear refraction index for the measured Z-scan traces. Once the value of N for the used flat-topped beam is determined, the relationship between T_{PV} and Φ_0 will become known (for instance, from Fig. 5). When a T_{PV} value is obtained from the experimentally measured Z-scan trace, we easily find the value of Φ_0 or γ (for instance, from Fig. 5). Of course, in order to confirm the reliability of the obtained result, we can use this value of Φ_0 to calculate the Z-scan trace and to compare with the measured Z-scan trace.

4 Conclusion

We present a theoretical investigation on the enhanced sensitivity of the flat-topped beam Z-scan scheme. The results reveal that the flat-topped beam Z-scan scheme can have higher sensitivity than the Gaussian beam Z-scan scheme. Some salient features of the flat-topped beam Z-scan traces are discussed. We also explore the flat-topped beam Z-scan traces under the excitation of CW laser, and Gaussian- and hyperbolic-secant temporal laser pulses, respectively. The flat-topped beam Z-scan technique should be a promising tool for characterizing the optical nonlinearity.

Acknowledgement This work was supported by the 973 Program under Grant No. 2006CB921805.

References

1. M. Sheik-Bahae, A.A. Said, E.W. Van Stryland, High-sensitivity, single-beam n_2 measurements. *Opt. Lett.* **14**, 955–957 (1989)
2. S. Hughes, J.M. Burzler, Theory of Z-scan measurements using Gaussian–Bessel beams. *Phys. Rev. A* **56**, R1103–R1106 (1997)
3. W. Zhao, P. Palffy-Muhoray, Z-scan technique using top-hat beams. *Appl. Phys. Lett.* **63**, 1613–1615 (1993)
4. B. Gu, J. Yan, Q. Wang, J.L. He, H.T. Wang, Z-scan technique for characterizing third-order optical nonlinearity by use of quasi-one-dimensional slit beams. *J. Opt. Soc. Am. B* **21**, 968–972 (2004)
5. W.Y. Zhang, M.G. Kuzyk, Effect of a thin optical Kerr medium on a Laguerre–Gaussian beam. *Appl. Phys. Lett.* **89**, 101103 (2006)
6. G.J. Lee, Z-scan method using the flat-topped beam and its application to the evaluation of the two-photon-absorbing material. *Jpn. J. Appl. Phys.* **42**, 3419–3423 (2003)
7. M. Alavinejad, B. Ghafary, F.D. Kashani, Analysis of the propagation of flat-topped beam with various beam orders through turbulent atmosphere. *Opt. Laser Eng.* **46**, 1–5 (2008)
8. C. Xie, R. Gupta, H. Metcalf, Beam profile flattener for Gaussian beams. *Opt. Lett.* **18**, 173–175 (1993)
9. W.B. Veldkamp, Laser beam profile shaping with interlaced binary diffraction gratings. *Appl. Opt.* **21**, 3209–3212 (1982)
10. J.A. Hoffnagle, C.M. Jefferson, Design and performance of a refractive optical system that converts a Gaussian to a flattop beam. *Appl. Opt.* **39**, 5488–5499 (2000)
11. S.D. Silvestri, V. Magni, O. Svelto, G. Valentini, Lasers with super-Gaussian mirrors. *IEEE J. Quantum Electron.* **26**, 1500–1509 (1990)

12. F. Gori, Flattened Gaussian beams. *Opt. Commun.* **107**, 335–341 (1994)
13. A.A. Tovar, Propagation of flat-topped multi-Gaussian laser beams. *J. Opt. Soc. Am. A* **18**, 1897–1904 (2001)
14. Y.J. Li, Light beams with flat-topped profiles. *Opt. Lett.* **27**, 1007–1009 (2002)
15. Y.J. Li, New expressions for flat-topped light beams. *Opt. Commun.* **206**, 225–234 (2002)
16. J.D. Gaskill, *Linear Systems Fourier Transforms and Optics* (Wiley, New York, 1978)
17. R.E. Samad, N.D. Vieira, Analytical description of Z scan on-axis intensity based on the Huygens–Fresnel principle. *J. Opt. Soc. Am. B* **15**, 2742–2747 (1998)
18. H.P. Li, B. Li, C.H. Kam, Y. L Lam, W.X. Que, L.M. Gan, C.H. Chew, G.Q. Xu, Femtosecond Z-scan investigation of nonlinear refraction in surface modified PbS nanoparticles. *Opt. Mater.* **14**, 321–327 (2000)
19. M. Sheik-Bahae, A.A. Said, T.H. Wei, D.J. Hagan, E.W. Van Stryland, Sensitive measurement of optical nonlinearities using a single beam. *IEEE J. Quantum Electron.* **26**, 760–769 (1990)